Proc. Natl. Acad. Sci. USA
Vol. 95, pp. 2039–2043, March 1998
Physics

Optimal modulation of a Brownian ratchet and enhanced sensitivity to a weak external force

MARTIN B. TARLIE* AND R. DEAN ASTUMIAN†‡

*James Franck Institute, University of Chicago, 5640 South Ellis Avenue, Chicago, IL 60637; and †Departments of Surgery and of Biochemistry, University of Chicago, 5841 South Maryland Avenue, Chicago, IL 60637

Communicated by Robert K. Adair, Yale University, New Haven, CT, November 24, 1997 (received for review June 15, 1997)

ABSTRACT **We studied the dynamics of a Brownian particle moving in a spatially anisotropic potential acted on by multiplicative temporal modulations so that $V(x,t) = g(t)U(x)$. Using the concept of the "thermodynamic action," we show that the class of modulation that maximizes the flow is a square-wave in time. We also show that adding a weak, homogenous force F in synergy with the square-wave modulation can cause particles of slightly different size to move in opposite directions. The synergetic change in velocity caused by F can be much greater than the drift velocity that would be caused by F alone.**

Motivated by the desire to understand energy transduction in biological systems (1, 2), recent attention has been devoted to the dynamics of particles moving in spatially anisotropic potentials that are fluctuating in time (for a recent review, see ref. 3). In addition to the biological motivation, there is interest in the potential technological use of such Brownian ratchets for the purpose of manipulating particles in colloidal suspensions (4–6). Typically, the system is under the influence of an external potential $V(x,t)$ and is in contact with an external bath that provides viscous damping of sufficient strength so that the inertia of the system is neglected. The system is described by a Langevin equation

$$\gamma\dot{x}(t) = -V'(x,t) + \sqrt{2\varepsilon}\eta(t), \qquad [1]$$

where γ is the coefficient of viscous friction, x is the coordinate of the center-of-mass of the particle, t is time, the prime denotes spatial differentiation, and the overdot denotes temporal differentiation. The noise strength ε is related to the temperature T and γ by the fluctuation dissipation relation: $\varepsilon = \gamma k_B T$, where k_B is Boltzmann's constant. Throughout this paper, we assume that the random forces are weak compared with the characteristic forces associated with V. Finally, $\eta(t)$ is Gaussian white noise.

Our focus is on multiplicatively modulated potentials (7–9) so that $V(x,t) = g(t)U(x)$, where $U(x)$ is an anisotropic ratchet potential (see, e.g., Fig. 1). In this case, the spatial average of the force is always zero. This is in contrast to the extensively studied (10–13) case of additive modulations where $V(x,t) = U(x) - xF(t)$, with $F(t)$ a fluctuating force with mean zero. For biological systems, which convert chemical energy into mass transport, multiplicative modulations are most relevant (14).

In this paper, we address the question: For a given potential $U(x)$, what is the optimal multiplicative temporal modulation $g(t)$ that maximizes the flow in one direction or the other? We show, by using path-integral methods, that the optimal class of modulation is a square-wave in time, and we provide a geometric means of determining the modulation within the class of square-waves that maximizes the flow. Furthermore, adding a small, homogenous, time-independent force can cause particles of slightly different size to move in opposite directions, thus allowing for a continuous separation process. The sensitivity of this system to the weak external force is enhanced strongly by the optimal modulation.

Paths of Least Action

Our approach is to consider the path integral expression for the conditional probability density $P(x_f,t_f|x_i,t_i)$ that is determined by summing over all paths that originate at the space-time point (x_i,t_i) and terminate at (x_f,t_f) (15–17). Each path is weighted by a factor $\exp(-S[x]/\varepsilon)$, where $S[x]$ is the thermodynamic action

$$S[x] = \frac{1}{4}\int_{t_i}^{t_f} dt(\gamma\dot{x}(t) + g(t)U'(x))^2 \qquad [2]$$

S is positive semi-definite (i.e., $S \geq 0$) so that optimal paths, which have maximum weight in the path integral, have zero action. Our goal is to find functions $g(t)$ that result in net flow and that allow for zero action paths that connect the local minima of U. Such modulations will thus be optimal.

We begin by examining the least-action paths for the unmodulated case, i.e., $g(t) = 1$. From this analysis, it will be evident how we then can modulate the system so as to create paths with zero action. For the potential $U_8(x)$ and taking $x_i = 0$ and $x_f = \pm L$, the least-action paths $x^{\pm}$ (see Fig. 2) were determined numerically by using an optimization algorithm based on Newton's method (18). The paths $x^{\pm}$ each can be decomposed into an uphill leg $x_u^{\pm}$ and a downhill leg $x_d^{\pm}$ with trajectories that approximately satisfy§

$$\gamma\dot{x}_u^{\pm} \approx +U'(x_u^{\pm}); \qquad \gamma\dot{x}_d^{\pm} \approx -U'(x_d^{\pm}), \qquad [3]$$

and that are valid for $t_f - t_i > t_a + t_b$ (19).

In Fig. 2, we see two characteristic time scales. The shorter, t_a, is the time required for a particle, with zero initial velocity, to slide a distance a down the steeper face of the potential, and the longer, t_b, is the time required to slide a distance b down the less steep face. From Eq. 3, we see that $t_a(\delta) = \gamma\int_{-\delta}^{-a+\delta} dx/U'(x)$, and $t_b(\delta) = \gamma\int_{\delta}^{b-\delta} dx/U'(x)$. Up to logarithmic corrections in δ, we have that $t_a \sim \gamma a^2/\Delta U$ and $t_b \sim \gamma b^2/\Delta U$, where $\Delta U \equiv U(b) - U(0)$.

Optimal Modulation

We learn from Eq. 3 inserted into Eq. 2 that for $t_f - t_i$ sufficiently long¶ only the uphill part of the path contributes to the action and asymptotically approaches ΔU as $t_f - t_i \to \infty$. The

The publication costs of this article were defrayed in part by page charge payment. This article must therefore be hereby marked "*advertisement*" in accordance with 18 U.S.C. §1734 solely to indicate this fact.

‡To whom reprint requests should be addressed.
§These approximate inequalities become exact in the limit that $T \to \infty$.
¶For $g(t) = 1$, S_c^+ and S_c^- are equal and are monotonically decreasing functions of $t_f - t_i$ that approach ΔU as $t_f - t_i \to \infty$.

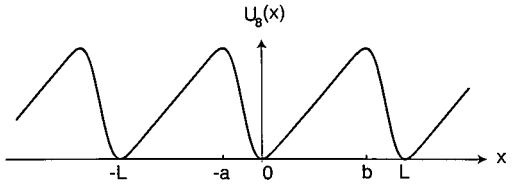

FIG. 1. Model potential $U_{8(x)}$ where $U_n(x) = U_n\Sigma_{i=1}^{n} e^{-I^2}/(n + 1)\sin(2\pi i(x - x_{n,0})/L)/i$.

contribution from the downhill path vanishes because for this path $\gamma\dot{x} = -U'$. To eliminate the nonzero contribution to the action, thereby creating an optimal path of zero action, we simply change the plus sign that appears in the first part of Eq. 3 to a minus sign. This can be accomplished if $g(t)$ is a function that switches between $+1$ and -1[‖] in a step-like manner so that

$$g(t) = \begin{cases} -1 & \text{for } n\mathcal{T} < t < n\mathcal{T} + \tau_- \\ +1 & \text{for } n\mathcal{T} + \tau_- < t < (n+1)\mathcal{T} \end{cases} \quad [4]$$

where $\mathcal{T} = \tau_+ + \tau_-$ is the period of the modulation, $\tau_-/\mathcal{T}$ is the fraction of the period during which $g = -1$, and n is any integer. This class of modulation (a square-wave) is optimal in the sense that there are zero action paths, i.e., paths for which the particle is always travelling downhill, that connect the local minima of U. Significantly, this modulation effectively eliminates diffusive steps, and in the limit that $\Delta U \gg k_B T$, the noise is relegated to the role of knocking the particles off of the potential maxima, with an equal probability to the right and left, when the potential is inverted.

Maximizing Flow

The problem that remains is to understand how the direction and magnitude of the flow depend on τ_+ and τ_-. Our goal is to locate the region(s) in the $\tau_- - \tau_+$ plane for which the flow is maximized. We begin by dividing the $\tau_- - \tau_+$ plane into eight regions as shown in Fig. 3. As a first step, we concentrate on how the direction of flow depends on the choice of parameters. It is easy to see that when $\tau_+ > \tau_-$, any flow that occurs must be to the left. It is always more probable for the particle to slide down the long leg of the potential (to the left) during the longer time period τ_+ than it is to slide down the long leg of the potential (to the right) during the shorter time period τ_-. An analogous argument, with the opposite conclusion, holds for the situation that $\tau_+ < \tau_-$. Thus, the current is antisymmetric with respect to reflection about the line $\tau_- = \tau_+$ so we need only consider $\tau_+ > \tau_-$.

We now focus on determining the region of the $\tau_- - \tau_+$ plane for which the flow is maximized. In region I of Fig. 3, the current is not appreciable because, on average, a particle initially located near $x = 0$ when g switches from $+1$ to -1 does not have enough time to reach $x = mL - a$ or $x = mL + b$ when the potential reinverts at $t = n\mathcal{T} + \tau_-$. (In the limit that $\tau_- = 0$, the flow is identically zero.) In region III, where $\tau_+, \tau_- > t_b$, the velocity is also essentially zero because now it is equally likely that the particle will make the excursion from $x = mL$ to $x = mL + b$ as to $x = mL - a$ in the time τ_-.

Now consider regions II and IV of Fig. 3. In region II, the particle has enough time, on average, to make the excursion from $x = mL$ to $x = mL - a$ in the time τ_- but not from $x = mL$ to $x = mL + b$. Thus, the velocity is determined by the transition probability from $x = mL$ to $x = (m-1)L$ in a time $\mathcal{T}$. This probability is $\approx 1/4$: a factor of $1/2$ from the splitting probability when the potential inverts at $t = n\mathcal{T}$ and another factor of $1/2$ when the potential reinverts at $t = n\mathcal{T} + \tau_-$. Thus, in this regime, the average velocity is $L/4\mathcal{T}$. In region IV, where $t_a < \tau - < t_b$ but $\tau_+ < t_b$, the dynamics is more complicated. When $g = -1$, the particle has enough time to execute a transition from $x = mL$ to $x = mL - a$ but not from $x = mL$ to $x = mL + b$. However, when $g = +1$, the particle does not have time to go all the way from $mL - a$ to $(m-1)L$, but because it makes more progress on this leg when $g = +1$ than when $g = -1$, it will eventually reach $(m-1)L$, so we still have net flow. In summary, the flow increases as the point (τ_-, τ_+) moves away from the regions $\tau - = 0$, $\tau_- = \tau_+$, and $\mathcal{T} = \infty$. Therefore, we expect that the maximum in the flow rate occurs near the boundary between regions II and IV.

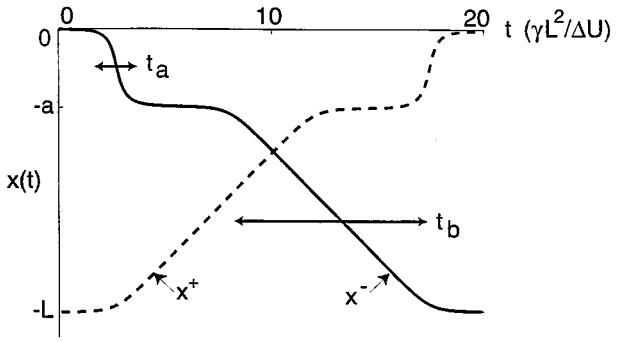

FIG. 2. Classical paths x^+ (dashed curve) and x^- (solid curve) as a function of t for $U_8(x)$ (see Fig. 1) with $t_f - t_i = 20$ and $\Delta t = 0.05$, where time is measured in units of $\gamma L^2/\Delta U$.

By performing Monte Carlo simulations of Eq. **1**, we confirm the general picture that is outlined above and summarized in Fig. 3. However, before continuing, we need to remark on the dependence of the flow properties on the noise: The flow is a nonmonotonic function of ε. As $\varepsilon \to 0$, the flow vanishes because the particle gets stuck in regions where the potential force $-U'$ vanishes. On the other hand, as $\varepsilon \to \infty$, the effect of the potential force becomes negligible and the dynamics becomes diffusion-like so that again the current approaches zero. Thus, there is a maximum in the flow for ε between the two extremes of zero and infinity. In what follows, our choice of ε coincides with this maximum.

The model potential used in the simulations is shown in Fig. 1. For $\varepsilon = 0.01\gamma\Delta U$, we numerically integrated Eq. 1 by using a forward Euler-differencing scheme. We computed the average velocity by integrating over 10^4 cycles of the modulation

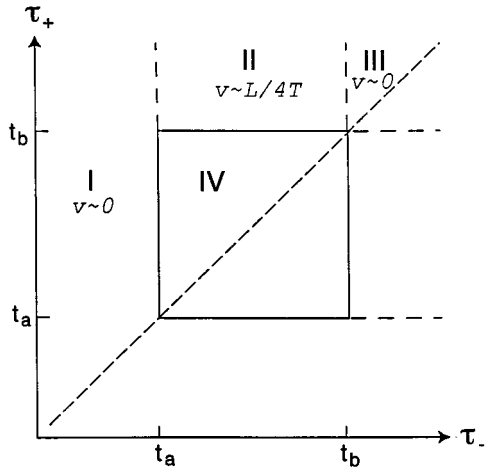

FIG. 3. $\tau_- - \tau_+$ plane divided into eight regions, four of which are labeled. The line $\tau_+ = \tau_-$ is a line of antisymmetry: When $\tau_+ < (>)\tau_-$, the velocity is positive (negative). The speed v is indicated for regions I–III.

[‖]In general, we could have taken g to switch between one positive and one negative constant. This alters t_a and t_b but does not affect the basic results.

and taking the ratio of the distance traveled to the duration of the excursion. Plotted in Fig. 4 is the absolute value of the average velocity as a function of τ_- and τ_+. Dark regions represent low velocities, and light regions represent high velocities. The maximal velocities plotted in Fig. 4 are approximately $L/(4T)$, as anticipated. These results confirm the picture described above. For a particle with a Stokes radius of 1 μm in water, $L = 10$ μm and $a = 1$ μm, and we get $L/(4T) \approx 2.5$ μm/s.

To summarize, we have shown that the optimal class of (multiplicative) modulation is a square-wave in time that switches between a positive and a negative constant and that within this class the velocity is maximum near the boundary between regions II and IV of Fig. 3. We determined the optimal class of modulation by identifying that these modulations allow for paths of zero action that connect the extreme points of $U(x)$. We then determined the sweet spot in the $\tau_- - \tau_+$ plane by using scaling arguments and the topological properties of the velocity in the $\tau_- - \tau_+$ plane. In addition, we confirmed the general conclusions by performing Monte Carlo simulations and by measuring the average velocity (see Fig. 4).

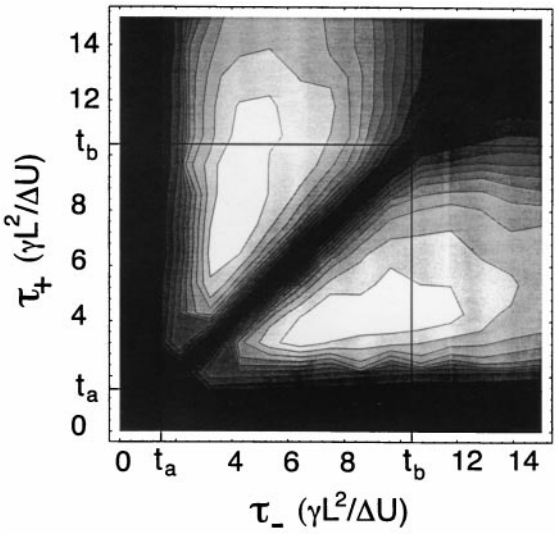

FIG. 4. Monte Carlo results for the absolute value of the average velocity as a function of τ_- and τ_+ for $n = 8$ ($a/b = 0.38$). The dark regions represent low velocity, and the light regions represent high velocity.

The Effect of a Homogeneous External Force

We now extend the previous model by adding a small force F that is constant in space and time. We will show that, under certain conditions, the ratchet can be extremely sensitive to very small forces. In addition, we will show that this sensitivity can be utilized to have particles of different size move in opposite directions—a phenomenon that is significant for particle segregation. An approximate formula for the velocity of a particle is

$$v = \frac{L}{T}\left(\frac{P^+}{n^+} - \frac{P^-}{n^-}\right). \qquad [5]$$

where $P^\pm$ is the probability that, if the particle starts at $x = 0$ at $t = 0_-$ (g switches at $t = 0$), the particle eventually ends up at $x = \pm L$ and $n^\pm$ is the number of cycles of the modulation that are required for this to take place. For simplicity of presentation, in what follows we restrict our attention to the regime where $\tau_+ > \tau_-$ and where $\tau_+ > t_b$ so that $n^+ = n^- = 1$**.

A weak homogeneous force has two significant effects. The first is that the splitting probabilities become different than 1/2. This is because the minima when $g = +1$ ($g = -1$) are shifted relative to the maxima when $g = -1$ ($g = +1$). Thus, when the potential switches, a particle initially at the bottom of a well finds itself slightly to the right or left of the maximum in the new configuration. The result is that, when $F \neq 0$, the splitting probabilities become (20)

$$q^-(F) = \frac{1}{2}\,\mathrm{erfc}\left(\frac{F}{\sqrt{2}W_s}\right), \qquad [6]$$

where

$$W_s = \sqrt{k_B T|U''(0)|} \qquad [7]$$

is an intrinsic force scale that determines the sensitivity of the splitting probability to an external force. The probability that the particle travels to the right is $q^+ = 1 - q^-$. We have approximated the potential in the region of the extrema as a parabola, and $U''(0)$ is the curvature at the maximum. Thus, Eq. **6** does not account for the asymmetry of the potential but should give an accurate estimate of the effect of F on the splitting probability in the regime where $k_B T \ll \Delta U$. For the potential shown in Fig. 1, $W_s \sim k_B T L^{-1}\sqrt{\Delta U/k_B T}$, where L is the period of U.

The second effect of the force is to change the sliding times. After the splitting has occurred, the center of mass of the probability distribution moves to the left or right at (essentially) a constant velocity that depends on the force F. The sliding times t_a and t_b are altered by a factor that depends on the direction of motion so that

$$t_\ell^\pm(F) = t_\ell(1 \pm F\ell/\Delta U)^{-1}, \qquad [8]$$

where + is for movement to the right and − is for movement to the left. In addition to the constant drift, the distribution spreads out at a constant rate that does not depend on the force. When $g = -1$, the probability $H^\pm_{\ell,g=-1}$ that the particle travels at least a distance ℓ to the left (−) or to the right (+) in the time τ_- can therefore be calculated, with the result that

$$H^\pm_{\ell,-1} = \frac{1}{2}\,\mathrm{erfc}\left(\frac{\pm F - F^*_\ell}{\sqrt{2}W}\right) \qquad [9]$$

where

$$F^*_\ell \equiv \frac{\Delta U}{\ell}\left(1 - \frac{t_\ell}{\tau_-}\right) \qquad [10]$$

and

$$W \equiv \sqrt{\frac{2\gamma k_B T}{\tau_-}}. \qquad [11]$$

Because we are treating the case that $\tau_+ > t_b$, when $g = 1$, the probabilities $H^\pm_{\ell,g=1}$ are approximately unity.

We are now in a position to determine the effect of F on the velocity. Eq. **5** is an expression for the velocity in terms of the probabilities $P_\pm$ and the average cycle times $n_\pm$. Because we have restricted our attention to values of $\tau_+ > t_b$, $n^+ = n^- = 1$ (21). The probabilities $P\pm$ for movement to the right (+) and left (−) are given by

$$P^+ = (q^+ H^+_{b,-1})\,(q^+ H^+_{a,1}) \qquad [12]$$

**Although we were able to obtain an approximate analytic formula for $v(\tau_-,\tau_+)$ in the entire $\tau_- - \tau_+$ plane, for clarity of presentation we have concentrated on the regime where n^+ and n^- are approximately unity.

and

$$P^- = (q^- H^-_{a,-1})\,(q^- H^-_{b,1}). \quad [13]$$

Using these formulae, we find that, for $\tau_+ > t_b$ and $\tau_+ > \tau_-$,

$$v(F) = \frac{L}{\mathcal{T}}\left((q^+)^2 H^+_{\ell,-1} - (q^-)^2 H^-_{\ell,-1}\right), \quad [14]$$

where we have used the fact that $H^{\pm}_{\ell,1} = 1$ in this regime. In Fig. 5, we compare the velocity from Monte Carlo simulations with the theory (*cf.* Eq. **14**). The $q_\pm$ functions are sensitive to forces centered around 0, with a width W_s, and the $H^\pm$ functions are sensitive to forces centered about F^*_ℓ with a width W. The key idea is that the velocity changes by $O(L/\mathcal{T})$ when F changes by $O(W)$ or $O(W_s)$. For optimal modulation, both W and W_s scale as $\sqrt{k_B T/\Delta U}$, so that if $\sqrt{k_B T/\Delta U} \ll 1$, then a small change in the force can cause a large change in the velocity. Thus, an optimally modulated ratchet acts as a mechanical analogue of an electrical transistor, where a small voltage can control a large current.

Technological Application

We now shift our attention to the potential application of these ideas to particle segregation. The ideal is for particles with different radii R to move in opposite directions at reasonable speeds, thereby forming the basis for a continuous (as opposed to batch) separation process. In the following discussion, we will show that, if the ratchet is operated in the appropriate manner and the appropriate force F is applied, it is possible to get particles of different size to move in opposite directions.

We begin by imagining that the ratchet is operating in a regime where $W_s > W$. In this case, as long as $F \leqslant W_s$, the splitting probabilities $q_\pm$ will be $1/2$ and essentially independent of F. Thus, examining Eq. **14**, we see that, for $\tau_+ > \tau_-$, the relevant sliding down times are t_a^- and t_b^+. Analogous arguments show that, for $\tau_+ < \tau_-$, the relevant sliding down times are t_a^+ and t_b^-. Using these results, we divide the $\tau_- - \tau_+$ plane in a manner analogous to that of Fig. 3, except now the relevant time scales are modified by the presence of F. In Fig. 6, we show this new division for $F > 0$. The key point is that the external force F breaks the anti-symmetry of the velocity about the line $\tau_+ = \tau_-$. The contour of zero velocity, shown in Fig. 6 as the thick black segments, is $\tau_- = (t_b^-/t_b^+)\tau_+$ for $\tau_+ < t_b^-$, and $\tau_- = t_b^+$ for $\tau_+ \geq t_b^-$. This means that particles of different size can have different contours of zero velocity. We can imagine, therefore, that, if the ratchet is operated in the region that lies between these zero-flux contours, the different-sized particles will travel in opposite directions.

The above argument relies crucially on the assumption that $W_s > W$; if this condition does not hold, then the division of the $\tau_- - \tau_+$ plane as shown in Fig. 6 is not valid. In this case, the effect of an applied force appears predominantly in the splitting probability (*c.f.* Eq. 6). The magnitude of this effect does not depend on the properties of the particles, so it is not possible to cause particles to move in opposite directions based on their size. Indeed, for $W > W_s$ there is no contour of zero velocity in the $\tau_- - \tau_+$ plane. Using Eq. **7** for W_s and Eq. **11** for W, the condition that $W_s > W$ is equivalent to $\sqrt{U''|(0)|} > \sqrt{2\gamma/\tau_-}$. But, because the zero flux contour is near $\tau_- = t_b$ (for small forces), we replace τ_- by $t_b = \gamma b^2/\Delta U$ in the above inequality and find that, for the potential shown in Fig. 1 and for $\tau_- = t_b$, the ratio $W_s/W \approx 4.4$. Thus, a continuous separation process, whereby particles of slightly different size move in opposite directions, is possible.

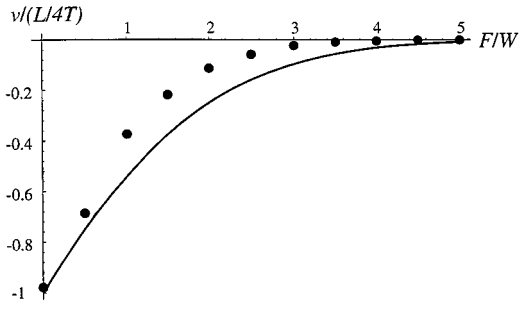

FIG. 5. Velocity v as a function of force F for $\tau_- = 0.9\,t_b$ and $\tau_+ = 1.4\,t_b$ and $\varepsilon = 10^{-4}$. The closed circles are simulation results, and the solid curve is obtained from Eq. 14.

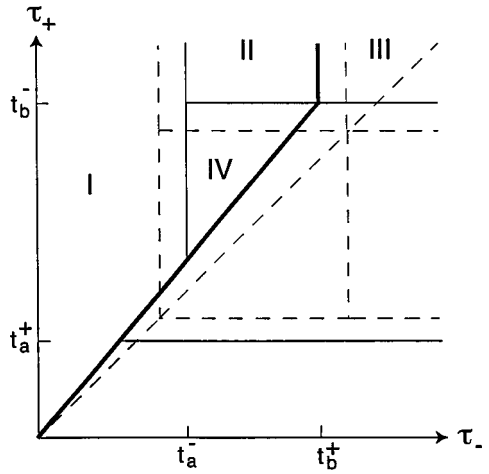

FIG. 6. Division of the $\tau_- - \tau+$ plane in the presence of a constant force $F > 0$. The sliding down times $t^{\pm}_{\mathrm{scrl}}$ are force-dependent, as described in the text, and the thick black line is the contour of zero flux.

Having seen how, in principle, it is possible to get particles of different size to move in opposite directions, we now show this explicitly. We imagine that we have a set of electrically charged particles, all with the same sign of charge. Consequently, in the absence of an external force, the square-wave modulation considered above has the property that $\tau_+ = \tau_-$ is a line of antisymmetry, independent of the size of the particle. Therefore, particles of different sizes may move at different speeds but not in different directions. However, as we have just seen, imposition of a macroscopic applied force F that is constant in space and time breaks this symmetry. The key idea is that the contour of zero flux, as indicated by the thick black line in Fig. 6, now curves upward (for $F > 0$). For $\tau_+ > t_b^-$, this zero-flux contour is given by $\tau_- = t_b^+(F)$. Thus, if $t_b^+(F)$ depends on the radius of the particle, then the velocity for particles of different size will change sign in different regions of the $\tau_- - \tau_+$ plane and, consequently, particles of different size can be made to move in opposite directions.

To see that $t_b^+ = t_b/(1 + Fb/\Delta U)$ depends on R recall that $t_b = \gamma b^2/\Delta U$. It is possible for γ, ΔU, and F to depend on R. First, according to the Stokes–Einstein formula, we have that $\gamma \sim R$. Second, if we assume that the ratchet potential is electrostatic in origin, then we can have $\Delta U \sim R^\alpha$ with $\alpha = 0$ (as may be appropriate for proteins) and $\alpha = 1,2$ [as may be appropriate for coloidal particles (21)]. Third, the macroscopic force F can scale as R^β, with $\beta = \alpha$ if F is electrostatic in origin or $\beta = 3$ if F is due to gravity. Thus, there are many possible combinations of α and β that will result in a dependence of t_b^+ on the radius R. The main conclusion, therefore, is that, under a wide variety of circumstances, it is possible to operate the ratchet in such a way that particles of different size will move in opposite directions.

To illustrate this we performed Monte Carlo simulations of Eq. **1** by using $U_8(x)$ for particles with $r = 1\ \mu$m and $r = 1.2\ \mu$m immersed in water at $T = 300$ K. We took $\gamma = 6\ \pi\zeta R$, where

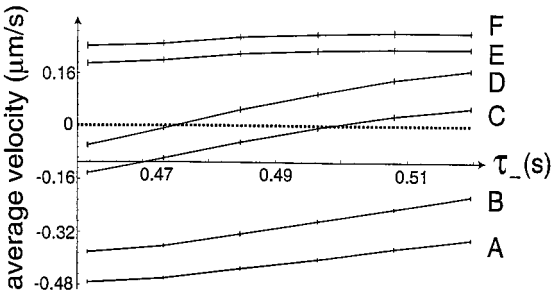

FIG. 7. Curve C: particle of radius $R = 1$ μm, density 1.05 g·cm^{-3}, in water at $T = 300$ K, subject to a constant force $F = 2.05 \times 10^{-15}$ N. Curves A, B, and D–F: $R = 1.2$ μm, $U \sim R^{\alpha}$, and $F \sim R^{\beta}$. A, $\alpha = 0$, $\beta = 0$; B, $\alpha = 0$, $\beta = 3$; D, $\alpha = 1$, $\beta = 3$; E, $\alpha = 2$, $\beta = 2$; F, $\alpha = 2$, $\beta = 3$. Average velocity as a function of τ_- for $\mathcal{T} = 0.46$ s.

$\zeta = 1$ cP is the viscosity of water, the ratchet force $-U'$ to be electrical with $\Delta U = 2000\, k_B T$ and $L = 4\ \pi\mu$m. The magnitude of F for the 1 μm-sized particle was 2.05×10^{-15} N, which is the net gravitational force that can be obtained by tilting the apparatus by 90°. As shown in Fig. 6, the contour of zero flux for $F > 0$ curves upward and roughly hugs the line $\tau_- = t_b^+$. Thus, if the ratchet is operated near the border between regions II and III, particles of different size will move in opposite directions. This is shown in Fig. 7, where we plot the average velocity v as a function of τ_- for $\mathcal{T}^{-1} = 2.2$ Hz for various combinations of α and β. In all cases, there are values of τ_- for which the 1 μm- and 1.2 μm-sized particles travel in opposite directions.

Summary and Conclusion

In summary, we have sketched out a conceptual framework for understanding how to optimize the velocity of a small particle induced by deterministic modulation of a ratchet potential. This provides a firm theoretical base for the two main results of this paper. (*i*) A weak external force (e.g., gravity for a 1-μm latex sphere in water) in synergy with the optimal modulation can allow particles of slightly different size to move in opposite directions. This suggests approaches for implementation of continuous separation techniques for microscopic particles and biopolymers. And (*ii*) The sensitivity to the weak external force is enhanced by the optimal modulation, thus allowing a weak force to control a large current—a mechanical analogue of a transistor.

We thank Eli Ben-Naim, Martin Bier, Imre Derenyi, Sue Coppersmith, Leo Kadanoff, Jiri Maly, and Tom Witten for helpful discussions and comments. This work was supported in part by the Materials Research Science and Engineering Centers Program of the National Science Foundation (DMR-9400379) (to M.B.T. and R.D.A.), and National Institutes of Health Grants R29ES06620 and RO3ES08913 (to R.D.A.).

1. Astumian, R. D., Chock, P. B., Tsong, T. Y., Chen, Y. & Westerhoff, H. V. (1987) *Proc. Natl. Acad. Sci. USA* **84,** 434–438.
2. Astumian, R. D., Chock, P. B., Tsong, T. Y. & Westerhoff, H. V. (1989) *Phys. Rev. A At. Mol. Opt. Phys.* **39,** 6416–6435.
3. Astumian, R. D. (1997) *Science* **276,** 917–922.
4. Rousselet, J., Salome, L., Ajdari, A. & Prost, J. (1994) *Nature (London)* **370,** 446–448.
5. Faucheux, L. P., Bourdieu, L. S., Kaplan, P. D. & Libchaber, A. J. (1995) *Phys. Rev. Lett.* **74,** 1504–1507.
6. Bier, M. & Astumian, R. D. (1996) *Phys. Rev. Lett.* **76,** 4277–4280.
7. Ajdari, A. & Prost, J. (1992) *C. R. Acad. Sci. Paris* **315,** 1635–1639.
8. Astumian, R. D. & Bier, M. (1994) *Phys. Rev. Lett.* **72,** 1766–1769.
9. Chawin, J. F., Ajdari, A. & Prost, J. (1995) *Europhys. Lett.* **32,** 373–378.
10. Magnasco, M. (1993) *Phys. Rev. Lett.* **71,** 1477–1481.
11. Bartusek, R., Reimann, P. & Hänggi, P. (1996) *Phys. Rev. Lett.* **76,** 1166–1169.
12. Luczka, J., Bartussek, R. & Hänggi, P. (1995) *Europhys. Lett.* **31,** 431–435.
13. Doering, C. R., Horsthemke, W. & Riordan, J. (1994) *Phys. Rev. Lett.* **72,** 2984–2987.
14. Astumian, R. D. & Bier, M. (1996) *Biophys. J.* **70,** 637–653.
15. Onsager, L. & Machlup, S. (1953) *Phys. Rev.* **91,** 1505–1511.
16. Stratonovich, R. L. (1972) *Am. Math. Soc.* **15,** 273–286.
17. Graham, R. (1973) in *Springer Tracts in Modern Physics*, ed. Höhler, G. (Springer, Berlin), Vol. 66, pp. 1–97.
18. Zhu, C., Byrd, R. H., Lu, P. & Nocedal, J. (1994) Technical Report (Electrical Engineering and Computer Science Department, Northwestern University, Chicago).
19. Luckock, H. & McKane, A. (1990) *Phys. Rev. A At. Mol. Opt. Phys.* **42,** 1982–1990.
20. van Kampen, N. G. (1990) *Stochastic Processes in Physics and Chemistry* (North-Holland, Amsterdam), Chap. XI.
21. Crocker, J. C. & Grier, D. G. (1996) *Phys. Rev. Lett.* **77,** 1897–1900.